

# Vitamin D<sub>3</sub> - A Structural Elucidation Example Using the Agilent 400-MR

## White Paper

### Author

Jarrett J. Farias  
Agilent Technologies, Inc.  
Santa Clara, CA USA

### Abstract

Vitamin D<sub>3</sub>, or cholecalciferol, is one of a group of related compounds that form the Vitamin D group of secosteroids. Determining the structure of Vitamin D<sub>3</sub> is a particularly interesting challenge – there are several functional groups, rings and stereochemical characteristics. The ease with which the Agilent 400-MR can acquire and process the data, including demanding experiments, makes this the spectrometer of choice for structure elucidation problems.



**Agilent Technologies**

1. Introduction .....	3
2. 1-D Proton ( <sup>1</sup> H) Spectrum.....	5
3. 1-D <sup>13</sup> C Spectra.....	7
4. Determine the number of and type of <sup>13</sup> C's (C, CH, CH <sub>2</sub> , CH <sub>3</sub> ) .....	9
5. Determine the direct <sup>1</sup> H- <sup>13</sup> C connectivities - Heteronuclear Single- Quantum Coherence (HSQC).....	10
6. Determine the <sup>1</sup> H spin systems and coupling networks - gradient COrrrelation SpectroscopY (gCOSY).....	13
7. Determine the <sup>1</sup> H spin systems and coupling networks - TOtal Correlation SpectroscopY (TOCSY) and gradient Heteronuclear Single-Quantum Coherence TOtal Correlation SpectroscopY (gHSQC-TOCSY) .....	16
8. Determine the long-range <sup>1</sup> H- <sup>13</sup> C connectivities - gradient Heteronuclear Multiple Bond Coherence (gHMBC) .....	19
9. Assigning stereochemistry - Rotational Overhauser Effect SpectroscopY (ROESY) .....	21
10. Conclusion .....	23

## 1. Introduction

The Agilent 400-MR excels not only for chemical confirmation and quantitation, but also in the ease of use of modern 1-D and 2-D NMR techniques used to map out atom-by-atom connectivity. This process can yield 3-dimensional molecular structure and stereochemistry for both small organic and inorganic molecules as well as larger peptides and proteins. The 400-MR is equipped with DirectDrive and DirectDigital RF architecture, ensuring optimal data quality for every sample, with push button simplicity even when using the most demanding experiments. Thus, the 400-MR is, by design, an easy to use NMR spectrometer that allows the organic chemist access to excellent NMR data.

This white paper takes you through a comprehensive example on how a complete 3-dimensional structure can be accomplished, using the 400-MR.

To make the work flow even more straightforward, the Agilent MR workstation software, VnmrJ 2.2 provides an intuitive interface for queuing sample acquisition, called StudyQ (Figure 1). Experiments such as those described in this detailed structure determination section can each be selected from tabs using a single mouse click. A group of selected experiments is automatically linked together in a queue.



Figure 1. The StudyQ provides an intuitive interface for queuing sample acquisition. A variety of 1-D and 2-D experiments can be selected by clicking on the name in the top left panel. The experiment then drops into the queue (bottom left). Experiments can be reprioritized within the queue.

Experiments can then easily be added to, deleted from, or rearranged within the queue, and the final queue can be submitted to the spectrometer for data acquisition.

In addition, complete parameter panels (Figure 1, bottom right) for each experiment are available. These provide a pre-optimized experimental setup that allows data collection without the need to be an expert in NMR. If

desired, the experimental panels also allow parameter optimization for each experiment and can be used to fine tune data acquisition, for example, for samples available in particularly small volumes.

After data acquisition, the data processing interface of the VnmrJ 2.2 software offers an impressive array of tools for data processing, manipulation and viewing. ViewPorts (Figure 2) are the actual spectra visualization areas that contain these tools.

One or more ViewPorts can be enabled with the push of a button. Using this feature, multiple spectra can be displayed side by side so that the data from different experiments can be reviewed at the same time. In addition, cursors can be linked among ViewPorts enabling spectra to be scrutinized in context with other data sets. Push pins allow text panels to be moved to one side and easily retrieved when needed (Figure 2). This allows the full screen to be used for graphics – which makes visualization, especially of 2-dimensional spectra substantially easier. Data processing icons are ViewPort sensitive, automatically shifting to the ViewPort of focus, providing an intuitive environment for the novice or inexperienced user.

All of the data in this white paper were collected using a standard Agilent 400-MR, equipped with an Automated Triple Broadband (ATB) probe. This probe is an excellent choice for high-throughput or ease-of-use laboratory environments, as it provides a very high degree of solvent flexibility. The probe yields optimal results without tuning when changing from, for example, DMSO, to methanol. It is capable of many experiments for chemical samples, offering both high frequency ( $^1\text{H}$  and  $^{19}\text{F}$ ) and low frequency (X tunable from  $^{15}\text{N}$  -  $^{31}\text{P}$ ) observe and decouple with minimal mechanical action.

Automated deuterium gradient shimming (Figure 3) was used throughout, enabling optimal data quality with minimal operator interaction. In fact, all other calibrations

such as lock, acquisition, power settings, and tip angles, all of which contribute to the excellent performance of the 400-MR, typically occur automatically within the experiment.

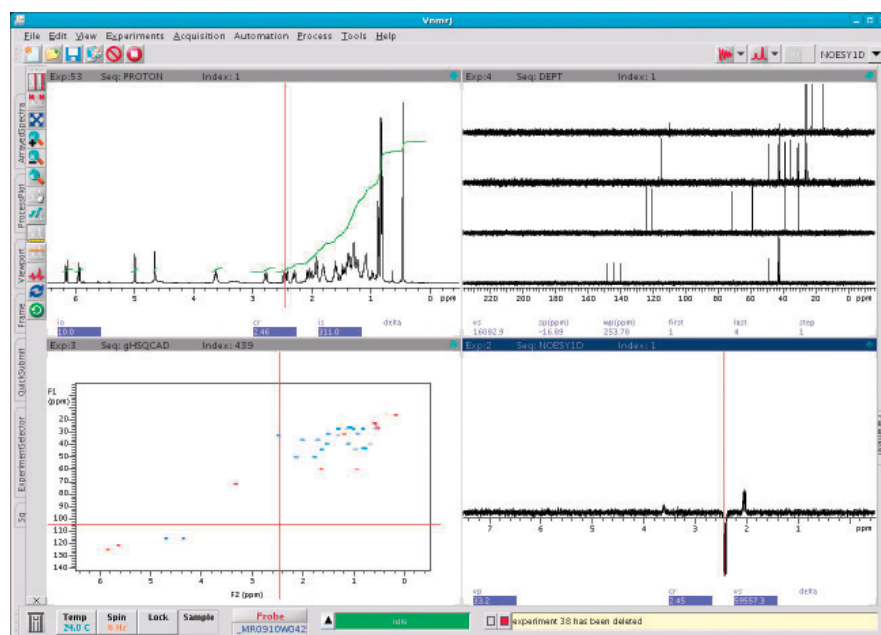


Figure 2. ViewPorts offer peak picking, integration, insets, annotation and other tools to manage the content and layout of spectra.

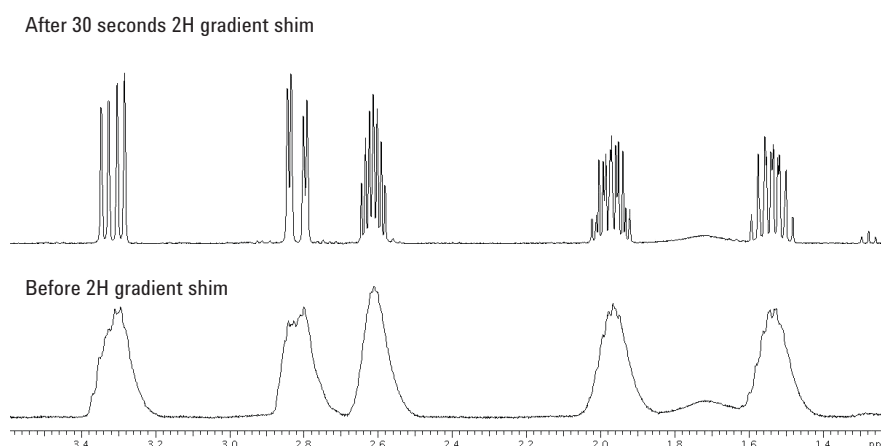


Figure 3. Results obtained using gradient shimming on a  $\text{CDCl}_3$  solution with an ATB probe. Best lineshape can be achieved in a very short time (30 seconds for this example).

The sample chosen for this structural elucidation had a concentration of 25 mg/600  $\mu\text{L}$ , in  $\text{DMSO-d}_6$ . The steps required to generate a complete 3-dimensional molecular structure comprise the following group of general experimental capabilities:

- **Find out the number of protons and a general understanding of the functional groups**

1-Dimensional (1-D)  $^1\text{H}$  spectra can provide integrals to find relative proton quantities, chemical shift to provide functional group information, and proton-proton couplings to find through-bond neighbors.

- **Specify the functional groups more thoroughly**

1-D  $^{13}\text{C}$  spectra, will confirm functional groups. DEPT will determine the number of, and type of  $^{13}\text{C}$ s ( $\text{C}$ ,  $\text{CH}$ ,  $\text{CH}_2$ ,  $\text{CH}_3$ ) by correlating carbon atoms to directly attached protons.

- **Determine the  $^1\text{H}$  coupling networks, that is, map chains of adjacent protons**

1-D and 2-D  $^1\text{H}$  correlation experiments, including gCOSY and TOCSY are techniques that enable more complete assignment of through-bond neighbors through additional resolution of proton-proton spin couplings.

- **Determine the short and long-range proton-carbon connectivities to improve knowledge of networked atoms**

2-D  $^1\text{H}$ - $^{13}\text{C}$  correlation experiments, such as gHSQC and gHMBC, assign carbon-proton couplings from one to several bonds distance.

- **Determine the 3-dimensional structure and stereochemistry**

1-D and 2-D nOe experiments, including ROESY provide through-space proton-proton interactions.

## 2. 1-D Proton ( $^1\text{H}$ ) Spectrum

Each nucleus being observed in a molecule, in this case a proton, resonates at a slightly different frequency because each exists in a slightly different electronic (and chemical) environment. The term chemical shift is used to describe this phenomenon.

All magnetic nuclei interact with neighboring magnetic nuclei through the bonding electrons, creating measurable spin couplings to each other, called coupling constants. This effect produces a specific pattern, called a splitting pattern.

The total absorption in a spectrum is directly related to the total number of nuclei doing the absorbing. Thus, the area under each peak (its integration) is proportional to the number of protons generating that peak relative to other peaks. These three pieces of information, that:

- Different nuclei in a system can be identified individually through chemical shift,
- The proportion of each type of nucleus is quantifiably measurable,
- Interactions between neighboring atoms can be identified,

is what makes NMR stand out compared to other analytical techniques.

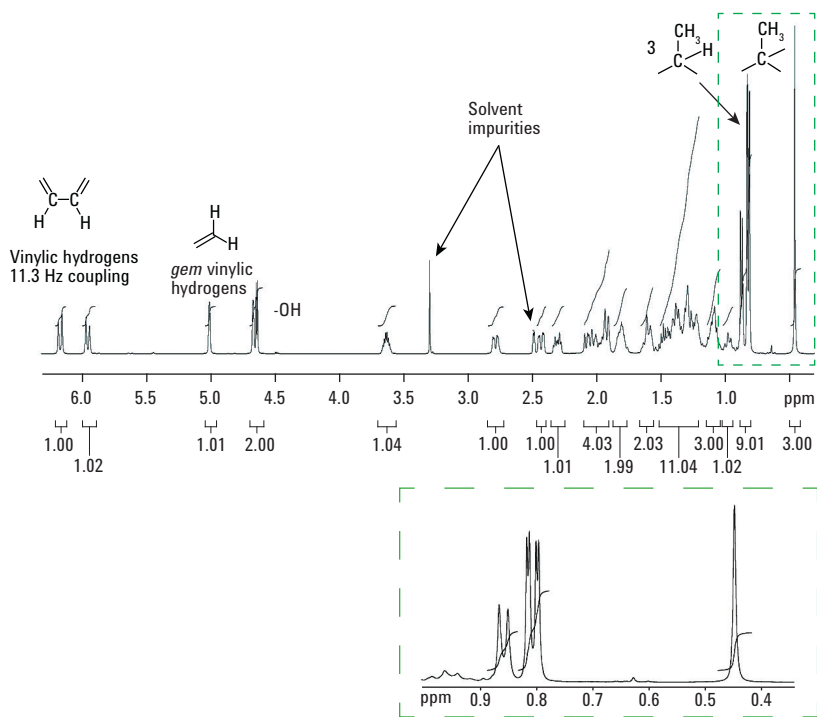


Figure 4.  $^1\text{H}$  spectrum showing major functional groups. High quality spectra such as this are easily obtained with the Agilent 400-MR. Note the flat baseline, attributable to the DirectDigital Receiver. The expansion of the methyl region in the green box shows how well such closely related structural elements are separated.

For this compound, the  $^1\text{H}$  spectrum (Figure 1) provides an integral total of 44 protons (or a multiple of 44), as each proton resonance must integrate to a whole number.

As we inspect the region from 6.5–2.2 ppm, we can start to identify characteristics of the peaks and plausible chemical environments. The peaks at 3.3 ppm and 2.5 ppm are due to HOD and DMSO- $d_6$ , impurities in the solvent used to dissolve the compound, information gathered from running a solvent blank.

The doublet at 4.64 ppm was seen to disappear with the addition of  $\text{D}_2\text{O}$ , implying it is an exchangeable proton. The chemical shift of 4.64 ppm indicates that this peak is most likely to be attributable to an alcohol. The multiplet at 3.62 ppm occurs at a chemical shift appropriate for a proton adjacent to an oxygen, and as the addition of  $\text{D}_2\text{O}$  caused the peak at 4.64 ppm to disappear, it also caused the splitting pattern to change for the multiplet, again in agreement of this assignment.

The two doublets at 6.13 and 5.92 ppm show coupling to each other, and appear in the region generally attributed to vinylic protons. The two protons at 4.98 and 4.64 ppm appear to be from *gem* vinylic protons.

As we inspect the region from 2.2–0.3 ppm, the only distinctive features are the singlet at 0.45 ppm, and three doublets at 0.86, 0.81 and 0.80 ppm. They are assigned as methyl groups based on their integration ratio of 3 and their chemical shift. We can further state that the methyl at 0.45 ppm is a tertiary methyl, having no protons adjacent to it (it is a single peak with no splitting pattern). The remaining methyls are secondary methyls, having 1 proton coupled to each as evidenced by the observable splitting of the resonance into two lines - doublets

### Here is what we know from inspection of the $^1\text{H}$ spectrum

We have several fragments of the molecule defined; we know there are 44 protons, 1 oxygen atom, and at least 12 carbon atoms. Several resonances are well defined, but a majority of resonances are overlapped in the region from 2.2–0.9 ppm. We have our first proposed molecular formula.

More information is required before significant headway can be made towards the goal of determining the structure of this compound. Reducing or eliminating the overlap of peaks seen in the  $^1\text{H}$  spectrum is a key step. This can be achieved in two ways. The first is to view spectra from nuclei (such as  $^{13}\text{C}$ ) that intrinsically provide improved breadth of chemical shift-increased dispersion. The second is to resolve overlapped 1-D spectra into additional dimensions, using spectra such as gCOSY and gHSQC are displayed in later sections.

Peak at (ppm)	Splitting pattern	Integral	Coupling constants (Hz)
6.13	d	1	11.3
5.92	d	1	11.3
4.98	br s	1	
4.64	d	1	2.2
4.61	d	1	4.5
3.62	octet	1	4.2
2.76	dd	1	12.6, 4.2
2.41	dd	1	13.1, 3.6
2.28	dt	1	4.9, 13.8
0.86	d	3	6.6
0.81	d	3	6.6
0.80	d	3	6.6
0.45	s	3	
1.64–0.9		17	
2.12–1.8		6	

d = doublet

br s = broad singlet

dd = doublet of doublets

s = singlet

### 3. 1-D $^{13}\text{C}$ Spectra

1-D carbon spectra also contain an abundant amount of information. We can determine how many different types of carbons are present, what type of electronic/chemical environment (neighboring nuclei) they have, and if obtained in quantitative conditions, how many of each type there are.  $^{13}\text{C}$  NMR is intrinsically insensitive and, generally,  $^1\text{H}$  interactions with the  $^{13}\text{C}$  nuclei are decoupled, collapsing multiplets into single lines for maximum sensitivity. Therefore, efficient decoupling as well as excellent lineshape are critical, as exhibited in both the  $^{13}\text{C}$  and DEPT spectra shown in Figure 5.

A quick inspection of the carbon spectrum (Figure 5) indicates 6  $\text{sp}^2$  carbons and one resonance around 68 ppm, confirming the alcohol moiety in the  $^1\text{H}$  spectrum. In order to collate the available information, such as the number of carbons present, we start counting (and labeling) from the left to right. There are 9 carbons from 150–50 ppm and 2 carbons from 20–10 ppm.

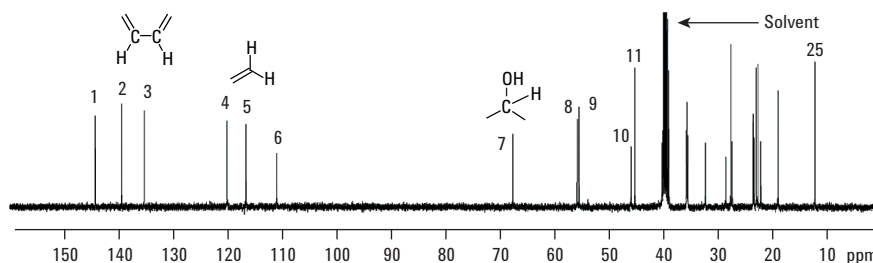


Figure 5.  $^{13}\text{C}$  spectrum showing major functional groups and numbering of the carbon atoms. Straightforward to acquire using an ATB probe,  $^{13}\text{C}$  data complements that gained from the  $^1\text{H}$  spectrum, Figure 4.

An expansion of the region between 50 to 20 ppm indicates 14 more carbons

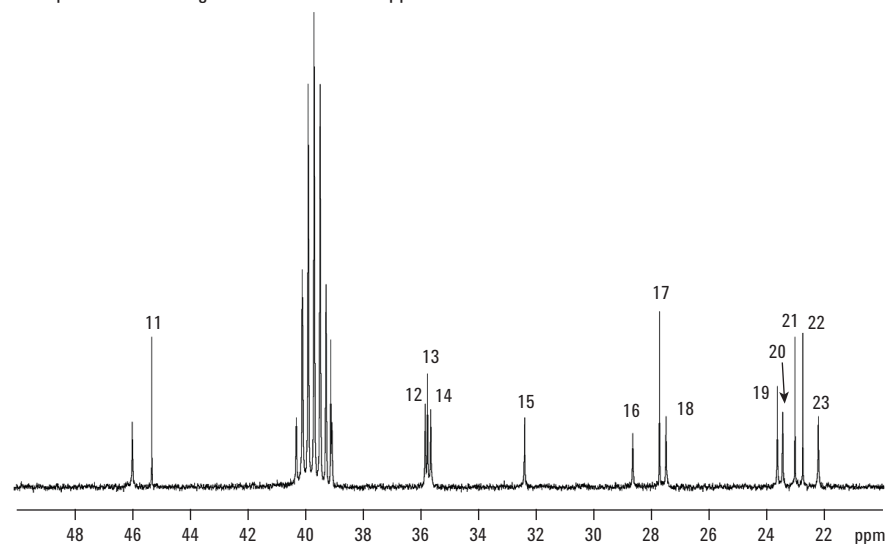


Figure 6. Expansion of the region 50–20 ppm of Figure 5. The strong resonance at ca. 40 ppm is due to the DMSO solvent.

Expansion around the solvent peak (Figure 7) provides an additional carbon resonance for a total of 26 carbons. The DMSO- $d_6$  carbon peak at 40.1 ppm is not as symmetrical as all the other DMSO- $d_6$  peaks. Adjusting the weighting functions before Fourier Transforming the data yields a 27th carbon resonance (Figure 8).

### Here is what we know from inspection of the $^{13}\text{C}$ spectrum

There are 27 carbon atoms, together with the 1 oxygen and 44 proton atoms to arrive at a working molecular formula of  $\text{C}_{27}\text{H}_{44}\text{O}$ . Sites of unsaturation is calculated to be six.

(number of Carbons  $\times$  2) minus number of Protons  $[\frac{1}{2} [(27 \times 2 + 2) - 44]]/2 = 6$

Three double bonds have already been accounted for, so the molecule must have three rings present.

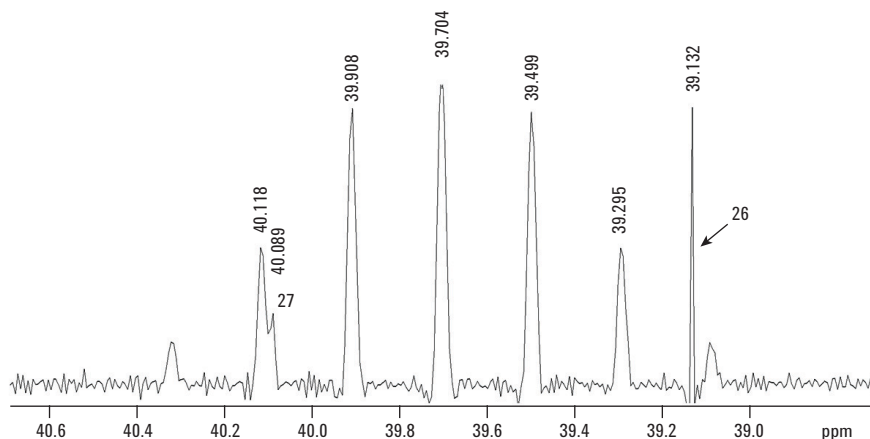


Figure 7. Adjusting the weighting function before Fourier Transformation yields a 27th carbon.

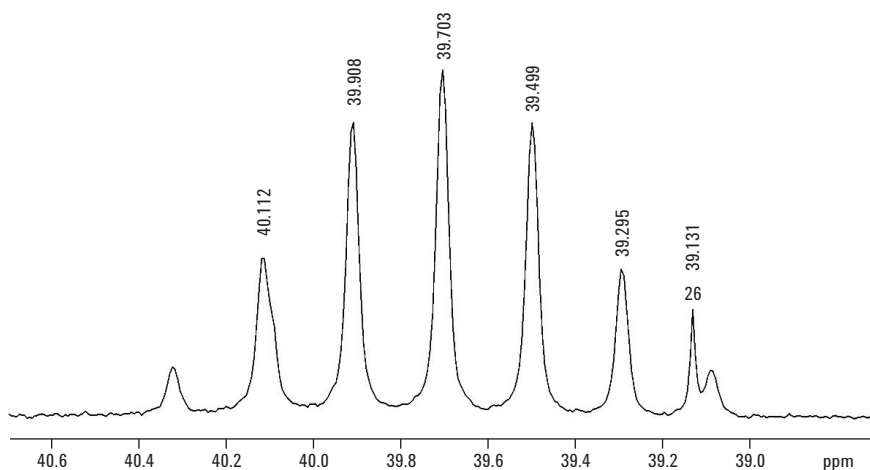


Figure 8. Further expansion of the  $^{13}\text{C}$  spectrum around the solvent resonance. Note the 26th carbon, labeled and the asymmetry of the line peak picked as 40.112 ppm.

$^{13}\text{C}$ Peak at (ppm)	Carbon number	$^{13}\text{C}$ Peak at (ppm)	Carbon number
145.56	C1	35.42	C15
140.56	C2	35.39	C16
136.38	C3	32.06	C17
120.89	C4	28.30	C18
117.36	C5	27.31	C19
111.70	C6	27.13	C20
67.76	C7	23.18	C21
55.86	C8	23.80	C22
55.50	C9	22.45	C23
45.85	C10	22.44	C24
45.20	C11	21.76	C25
39.83	C12	18.59	C26
38.90	C13	11.75	C27
35.63	C14		



#### 4. Determine the number of and type of $^{13}\text{C}$ 's (C, CH, $\text{CH}_2$ , $\text{CH}_3$ )

Along with the carbon spectrum, the multiplicity-edited DEPT spectra (Figure 9) show the populations of methine, methylene, and methyl resonances in the unknown compound.

It is important to note that information obtained from the DEPT experiment can also be obtained using **indirect detection techniques** that are introduced in the next section. Although indirect detection techniques offer an increase in sensitivity, thereby providing information on more dilute samples in a shorter amount of time, the DEPT experiment gives data that is very easily interpreted.

Of particular interest, is the way in which this experiment resolves the two peaks hidden by the  $\text{DMSO-d}_6$  signal (Figure 10) – which were alternatively resolved by using Fourier Transform weighting functions (Figure 7).

We now have all the building blocks needed put together a 2-dimensional structure. The next step in the analysis is to determine the direct  $^1\text{H}$ - $^{13}\text{C}$  connectivities before assembling the blocks.

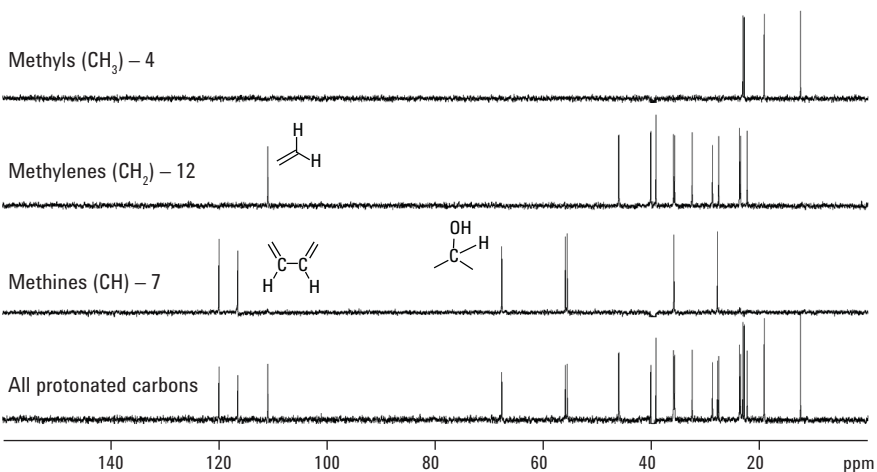


Figure 9. DEPT spectrum showing, from top down, protons attached to carbons as  $\text{CH}_3$ ,  $\text{CH}_2$  and CH moieties, with all protonated carbons, the sum of the spectra above it, at the bottom.

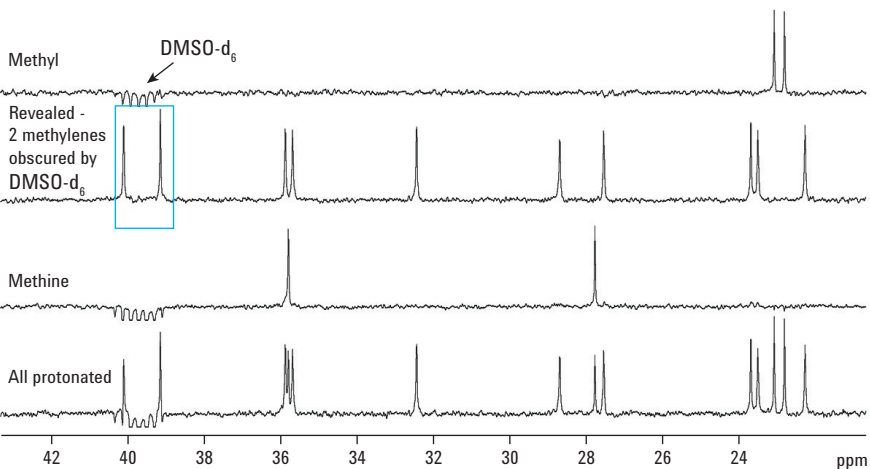


Figure 10. Expansion of solvent region of DEPT spectra. The two  $\text{CH}_2$  groups partially obscured by the solvent are highlighted.

### Here is what we know from inspection of the $^{13}\text{C}$ DEPT spectrum

We see 23 protonated carbon atoms, thus the unknown molecule has four quaternary, at 145.56, 140.56, 136.38, and 45.20 ppm. Furthermore, there are three carbons between 35.60 and 35.40 ppm, the center one of which is a methine.

Note that the  $^1\text{H}$  peaks and the  $^{13}\text{C}$  peaks are not correlated in this table, they are just laid out as lists.

### 5. Determine the direct $^1\text{H}$ - $^{13}\text{C}$ connectivities—Heteronuclear Single-Quantum Coherence (HSQC)

Proton-carbon connectivities are very easily assigned through the elegance of the gradient- HSQC (gHSQC) experiment. The gHSQC experiment provides not only basic  $^1\text{H}$ - $^{13}\text{C}$  one-bond correlations, it can also correlate as a function of proton multiplicity at each carbon site. One variation of the gHSQC experiment provides phase-sensitive information by displaying peaks arising from the  $\text{CH}_2$  sites as inverted with respect to the CH and  $\text{CH}_3$  peaks (same phase and opposite phase). The spectrum is read by identifying peaks relative to their vertically and horizontally corresponding chemical shifts (and spectra).

$^{13}\text{C}$ Peak at (ppm)	DEPT	Carbon number
145.56	C	C1
140.56	C	C2
136.38	C	C3
120.89	CH	C4
117.36	CH	C5
111.70	$\text{CH}_2$	C6
67.76	CH	C7
55.86	CH	C8
55.50	CH	C9
45.85	$\text{CH}_2$	C10
45.20	C	C11
39.83	$\text{CH}_2$	C12
38.90	$\text{CH}_2$	C13
35.63	$\text{CH}_2$	C14
35.42	CH	C15
35.39	$\text{CH}_2$	C16
32.06	$\text{CH}_2$	C17
28.30	$\text{CH}_2$	C18
27.31	CH	C19
27.13	$\text{CH}_2$	C20
23.18	$\text{CH}_2$	C21
23.80	$\text{CH}_2$	C22
22.45	$\text{CH}_3$	C23
22.44	$\text{CH}_3$	C24
21.76	$\text{CH}_2$	C25
18.59	$\text{CH}_3$	C26
11.75	$\text{CH}_3$	C27

The data shown in Figure 11 is a 2-D contour plot of the full gHSQC dataset. Note the sensitivity of the experiment, as tiny impurities are observed in the proton spectrum and inverse detected experiment, while no carbon is visible in the carbon observe spectrum. This shows the extreme sensitivity of running inverse detected experiments compared to direct X nuclei observe experiments.

Figure 12 shows an expansion of the direct  $^1\text{H}$ - $^{13}\text{C}$  correlations for the aliphatic region. Note the CH and  $\text{CH}_3$  correlations show multiple contours, while  $\text{CH}_2$  correlations show a single contour because they are inverted. Methyls can be easily determined from the integration of the  $^1\text{H}$  spectrum and correlating them to their respective carbon resonance. Of significance is C15, the methine that is between two methylene groups, 0.1 ppm apart (Figure 10, ca. 36 ppm). This methine has a relatively low signal intensity and does not appear as clearly as in the DEPT experiment, but is visible. The  $\text{DMSO-d}_5$  correlation also appears, and can be used to reference the spectrum.

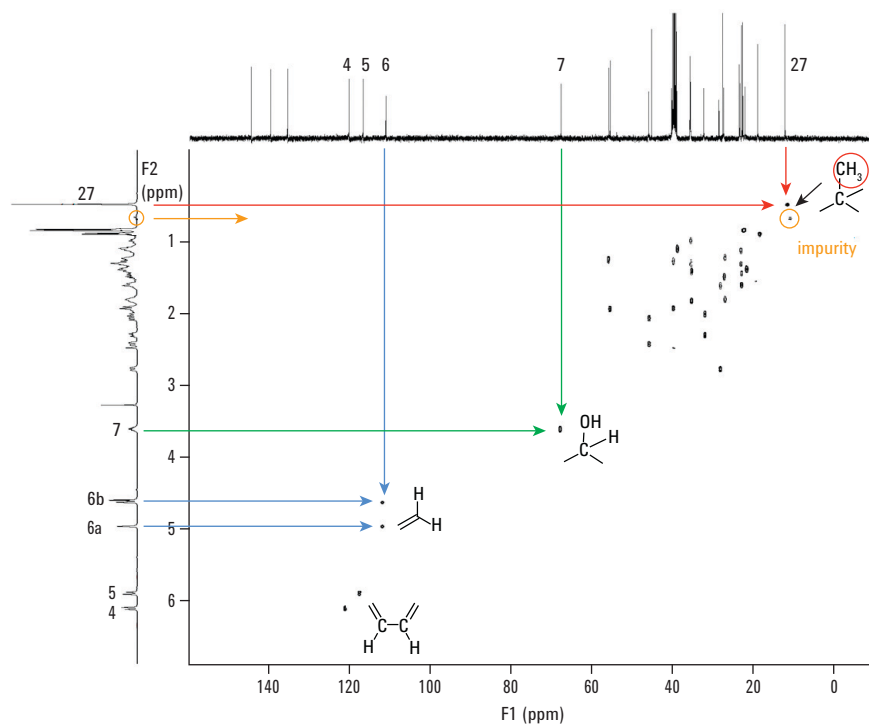


Figure 11. gHSQC data with arrows indicating correlations between specific carbon and proton signals.

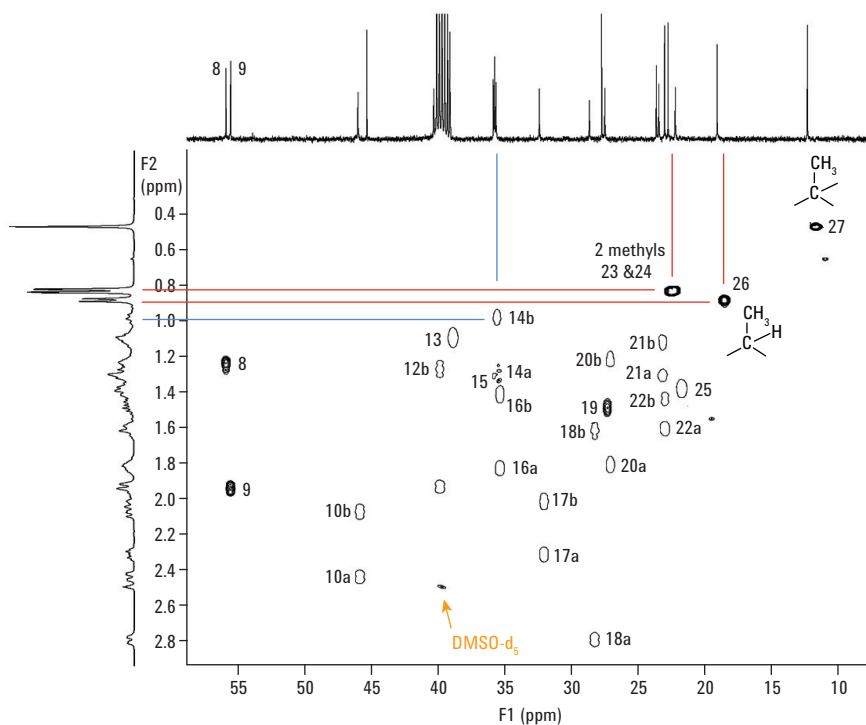


Figure 12. Expansion of the aliphatic region of the gHSQC experiment. Some correlations have been indicated and the methyls and methines (contoured) have been differentiated from the inverted methylenes by color coding.

### Here is what we know from inspection of the $^1\text{H}$ - $^{13}\text{C}$ gHSQC spectrum

We have now assigned all proton resonances to their corresponding carbon atoms and laid them out as connected groups in the table opposite.

We can make good use of the information provided in the gHSQC experiment to sort out the  $^1\text{H}$  coupling networks. In addition to telling us which protons are coupled to which carbon atoms, the gHSQC also tells us which protons are geminal pairs (for example, the peaks annotated as 10a and 10b in Figure 12). This information can be extended into the results provided by the COSY experiment (Figure 13).

Additional long range proton-carbon correlations can be performed by the gHMBC experiment, which will be discussed in section 8, Determine the long-range  $^1\text{H}$ - $^{13}\text{C}$  connectivities, gradient Heteronuclear Multiple Bond Coherence (gHMBC).

$^1\text{H}$ Peak at (ppm)	Number scheme	$^{13}\text{C}$ Peak at (ppm)	DEPT
	1	145.56	C
	2	140.56	C
	3	136.38	C
6.13	4	120.89	CH
5.92	5	117.36	CH
4.98	6a	111.70	CH <sub>2</sub>
4.64	6b		
3.62	7	67.76	CH
1.24	8	55.86	CH
1.91	9	55.50	CH
2.42	10a	45.85	CH <sub>2</sub>
2.07	10b		
	11	45.20	C
1.93	12a	39.83	CH <sub>2</sub>
1.27	12b		
1.10	13	38.90	CH <sub>2</sub>
1.31	14a	35.63	CH <sub>2</sub>
0.98	14b		
1.28	15	35.42	CH
1.82	16a	35.39	CH <sub>2</sub>
1.42	16b		
2.31	17a	32.06	CH <sub>2</sub>
2.02	17b		
2.80	18a	28.30	CH <sub>2</sub>
1.62	18b		
1.49	19	27.31	CH
1.81	20a	27.13	CH <sub>2</sub>
1.24	20b		
1.31	21a	23.18	CH <sub>2</sub>
1.12	21b		
1.61	22a	23.08	CH <sub>2</sub>
1.44	22b		
0.81	23	22.45	CH <sub>3</sub>
0.80	23	22.44	CH <sub>3</sub>
1.39	25	21.76	CH <sub>2</sub>
0.86	26	18.59	CH <sub>3</sub>
0.45	27	11.75	CH <sub>3</sub>
4.61	28		OH

## 6. Determine the $^1\text{H}$ spin systems and coupling networks gradient COrrelation SpectroscopY (gCOSY)

gCOSY is a common 2-D method for sorting out coupling networks by correlating protons that are scalar (through-bond)-coupled. Three gCOSY spectra are shown in Figure 13. From the first spectra, it is easy to see that  $^1\text{H}$ - $^1\text{H}$  couplings, and therefore connectivities, can be quickly deduced provided that there is sufficient data resolution or chemical shift separation. That is, this 2-D method provides improved peak dispersion compared to a congested 1-D proton spectrum.

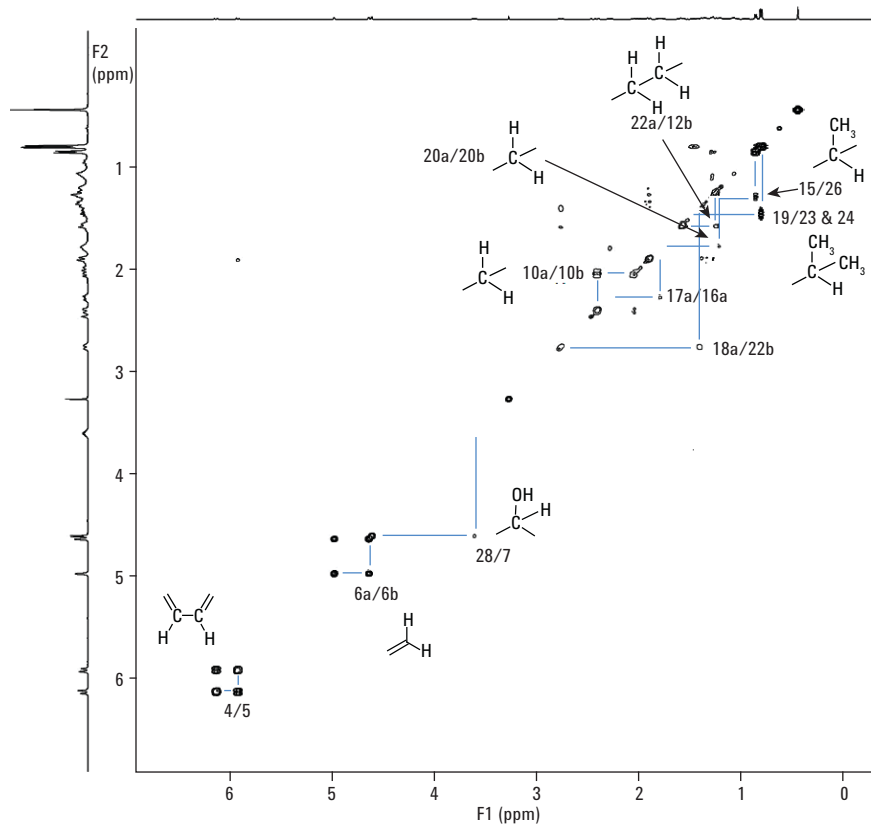


Figure 13. gCOSY spectrum showing well separated, easily correlated peaks.

The second spectrum, Figure 14, is of the same region as the first, but at a lower vertical threshold. Here we can see more than just geminal and vicinal correlations. Long-range couplings, those that involve more than three bonds, are common with allylic hydrogens and in compounds that are rigid bicyclic systems. These couplings, which are made possible through overlapping orbitals, usually have a stereochemical requirement. Alkenes often show small couplings (a maximum of  $4J = 3$  Hz) between protons substituted on carbons alpha to the double bond and those on the opposite end of the double bond. Saturated systems can exhibit long-range couplings through an arrangement of atoms in the form of a W ( $4J$ ), with protons occupying the end positions. Angular methyl groups in steroids, or those at the ring junctions in a decalin system, often exhibit peak broadening due to W coupling with several protons on the ring, causing broadening of the methyl resonance peak rather than definitive peak splitting. In addition to this long-range coupling, nuclei which are several atoms apart but which are close together spatially also may produce off-diagonal peaks.

The second spectrum allows us to deduce a larger substructure as shown on the left portion of Figure 14.

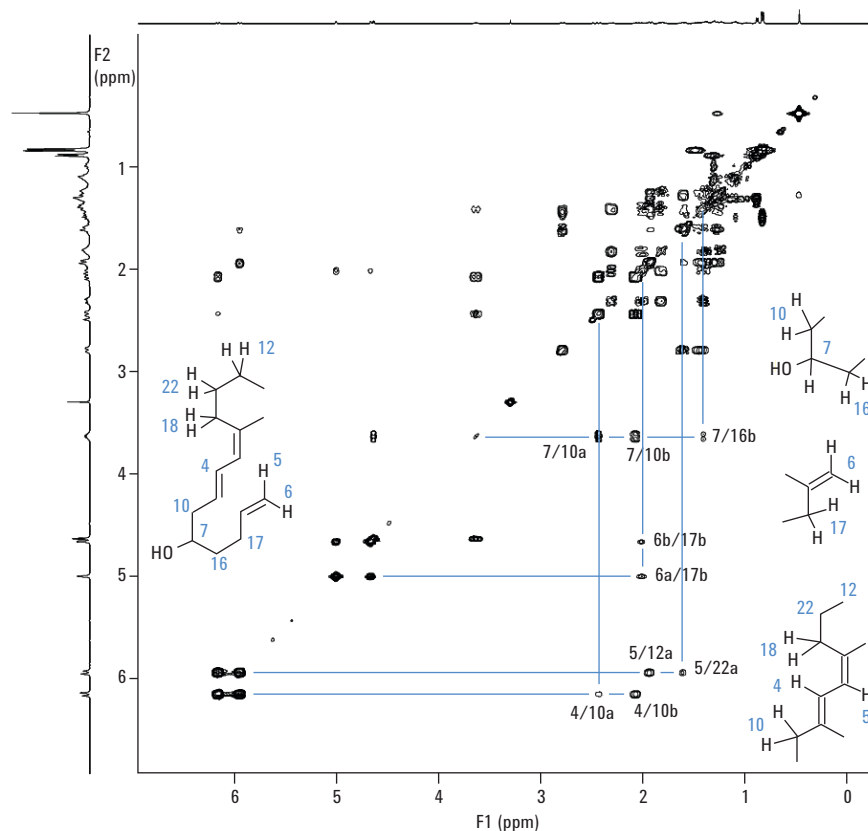


Figure 14. Lower threshold gCOSY plot showing more extensive correlations than Figure 13. The fragments shown to the right are grouped together on the left according to the known correlations. For example, protons numbered 10 are connected to that numbered 4 in the bottom right, and also to 7 and 16 in the top right, allowing us to join these two fragments. Additionally, from Figure 13, we know that 16 and 17 are connected. The correlation between 6 and 17 in this Figure allow us to link the upper and middle right fragments.

An expansion of the region between 0.3 and 3.8 ppm allows us to deduce two more substructures, shown at the top of Figure 15. However, this spectrum also demonstrates that congestion interferes with clear assignment of all the proton resonances. For assignment of overlapping resonances in such a spectrum, it is necessary to deconvolute the spectral region by using still more informative experiments that map out single resonance positions either by long range proton-carbon correlation spectroscopy or correlation within a proton coupling network, see Sections 7 and 8.

### Here is what we know from inspection of the $^1\text{H}$ - $^1\text{H}$ gCOSY spectrum

We have 21 of the 27 carbons associated with four larger substructures. The top three are accounted for by the data in Figures 14 and 15. The bottom substructure is at the top right of Figure 13.

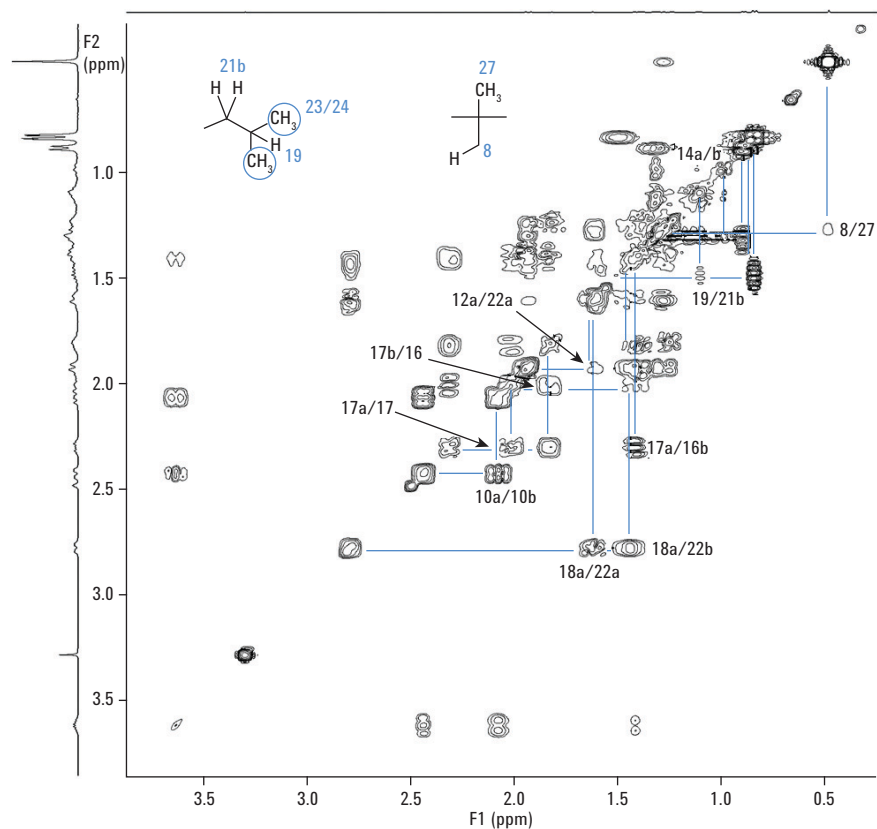
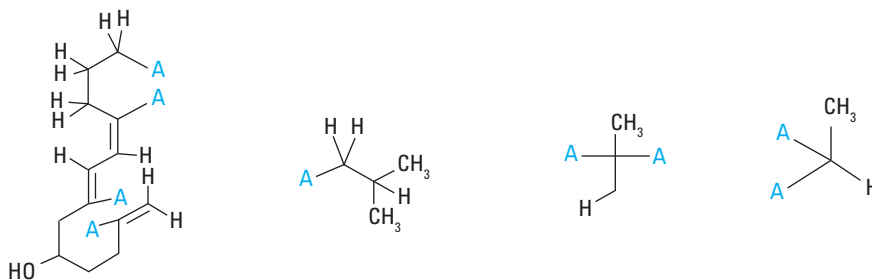


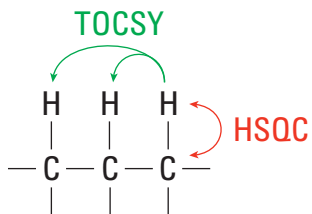
Figure 15. Additional expansion of the more highly congested region between ca. 0.3 and 3.8 ppm.

Long range couplings are present, common with allylic hydrogens and in rigid bicyclic systems, as well as providing insight to the molecule's stereochemistry. The singlet methyl has a long range correlation to a proton, suggesting an angular methyl group in a rigid bicyclic system due to *W* coupling.

Now, we can proceed to creating correlations within a proton coupling network which enables us to verify known actual connectivities and determine others which remain unknown, due to the complexity of certain spectral regions.



**7. Determine the  $^1\text{H}$  spin systems and coupling networks - T0tal Correlation SpectroscopY (TOCSY) and gradient Heteronuclear Single-Quantum Coherence T0tal Correlation SpectroscopY (gHSQC-TOCSY)**



Techniques such as TOCSY are 2-D experiments that determine complete proton spin systems by identifying protons belonging to the same scalar-coupling network.

This information helps us to assemble the various  $^1\text{H}$  spin networks into molecular fragments. In the TOCSY spectrum shown in Figure 16, the boxed region shows the doublet methyls and their correlations.

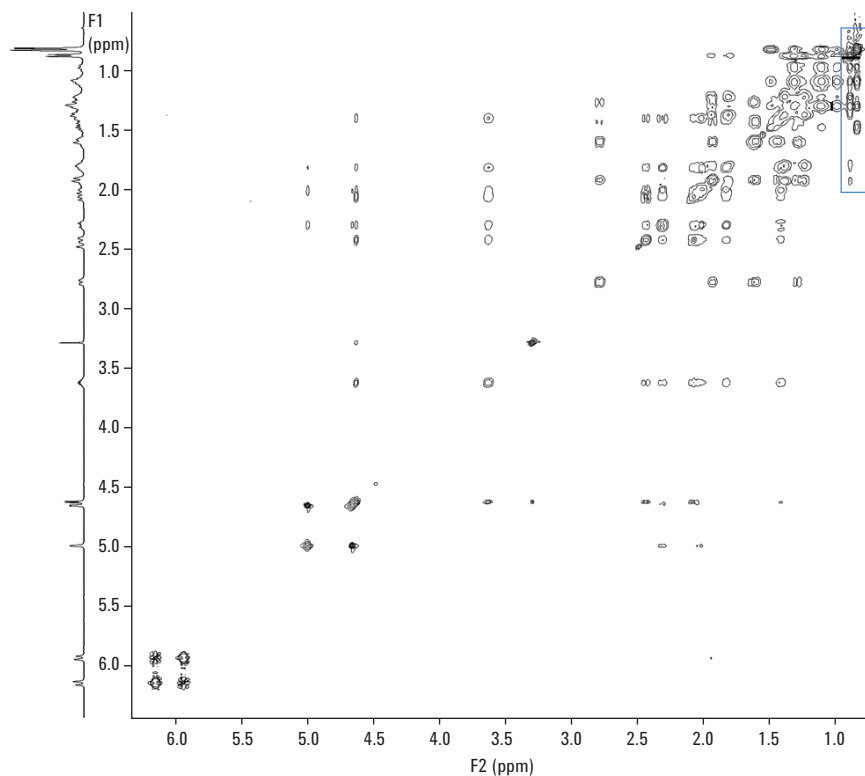


Figure 16. The boxed region shows the protons correlated to the doublet methyls, that is the protons that can couple to these methyls and, therefore, belong to the same fragment network.



An expansion of this region, Figure 17, indicates the basic units in this large spin system. Here, methyls 23 and 24 are part of the same spin system with methine 19, and methylenes 14 and 13. We do not clearly see the correlation to methylene 21, which was indicated in the gCOSY experiment, but it is clear that this experiment allows us to expand our knowledge of the spin system containing methyls 23 and 24 beyond that observed in the gCOSY experiment. The spin system of methyl 26 is also extended, from methine 15 to include methines 8 and 9, and methylenes 13, 14, 19, 20, and 25.

Therefore, it can be deduced, through the connectivities of methines 13 and 14, that the methyls are in the same fragment.

The gHSQC-TOCSY experiment provides  $^1\text{H} - ^1\text{H}$  coupling information with the increased dispersion of  $^{13}\text{C}$ . In the spectrum shown in Figure 18, we can see that methyl 26 has a long-range correlation to the methyls 23 and 24. Note the resolution in the carbon dimension which allows us to distinguish between methylenes 19 and 20. Overall, this spectrum is significantly less congested than the TOCSY spectrum.

The single 2-D TOCSY and gHSQC-TOCSY experiments are not capable of showing the order in which these fragments are linked together. While these 2-D experiments could be run with several mixing times to determine adjacent fragments, a 1-D TOCSY with an arrayed mixing time will provide this information at a fraction of the time needed for the 2-D experiments and at a higher resolution.

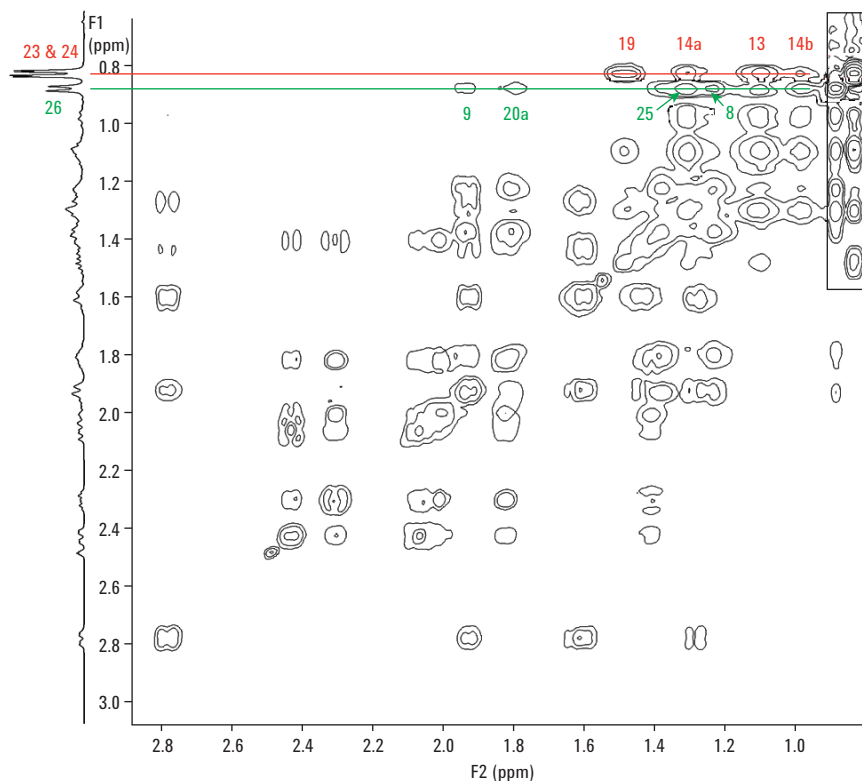


Figure 17. Expansion of the methyl region of Figure 16. Correlations for the methyls 23, 24, and 26 are shown.

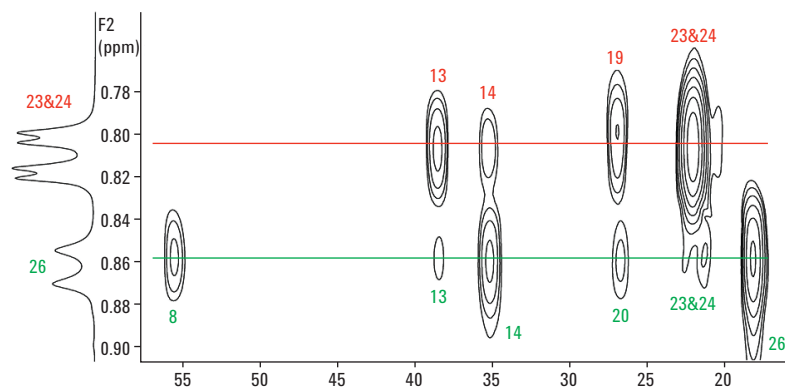


Figure 18. The  $^{13}\text{C}$  dimension of the gHSQC-TOCSY experiment allows clearer representation of the coupled methyl-containing network.

1-D TOCSY experiments benefit from the ability of a spectrometer to selectively irradiate particular regions of a spectrum. The use of pulsed field gradient techniques, such as the state-of-the-art experimental element **Double Pulsed Field Gradient Spin Echo** (DPFGSE), combined with fast and precise radiofrequency (RF) generation for selective excitation are easy with the Agilent 400-MR system. Intuitive software allows easy selection of the desired resonance or series of resonances. These capabilities are essential in order to obtain excellent results such as the 1-D TOCSY data presented here.

In the 1-D DFPGE-TOCSY experiment shown in Figure 19, the two methyl doublets at 0.8 ppm were selectively irradiated and acquired as an array of various mixing times. The resulting arrayed stacked spectra show the  $^1\text{H}$  spin system associated with each methyl doublet. As one moves up the stacked plots, it becomes clearly evident which basic units are next to each other. Methyls 23 and 24 are next to methine 19, which is next to methylene 21, which is connected to methylene 13, which is adjacent to methylene 14, which is connected to methine 15, which is then connected to methyl 26.

A similar experiment (Figure 20) was performed for the methyl at 0.86 ppm (methyl 26). In addition to seeing the reverse path, methine 15 was next to methine 8, which is next to methylene 20, which is next to methylene 25, which is adjacent to methine 9.

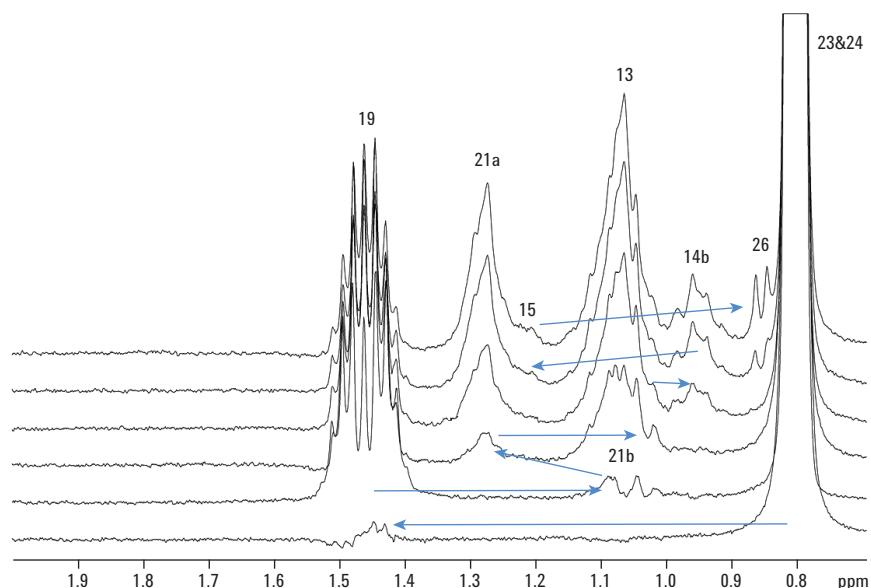


Figure 19. An array of mixing times allows the spin magnetism to propagate further through a network, creating a sequential pattern of growing peak intensity. Mapping the growth of various intensities against time provides a map of neighbors.

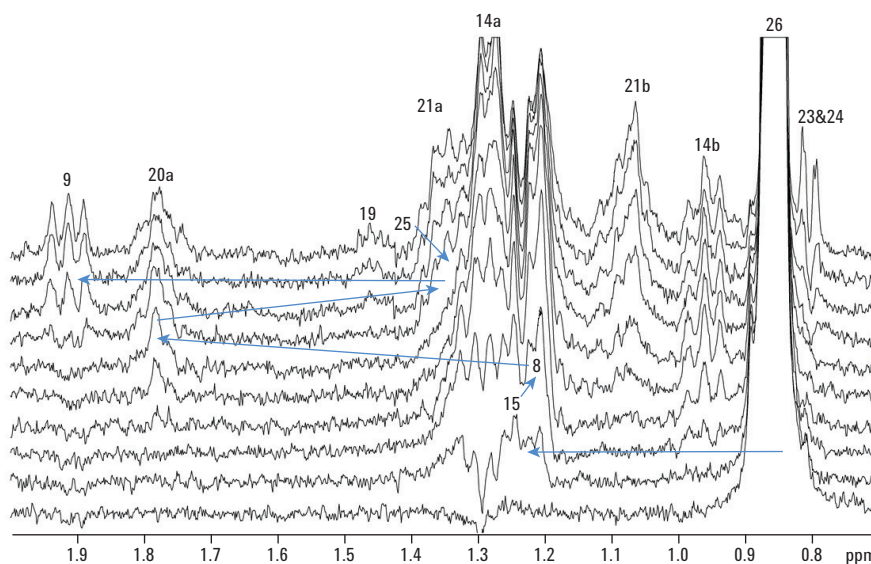
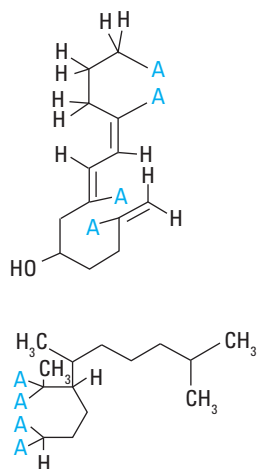


Figure 20. 1-D DFPGE-TOCSY arrayed from methyl 26, 0.86 ppm.

Compare the easy visualization of the spin systems for the methyls with the upfield, complex, overlapping resonance region in the 2-D gCOSY and 2-D TOCSY experiment in Figure 20. Also visible in Figure 20 is the additional information that methine 9 is a triplet. This peak overlaps with methylene proton 12a in the  $^1\text{H}$  1-D and gCOSY experiments.

### Here is what we know from inspection of the TOCSY types of experiments

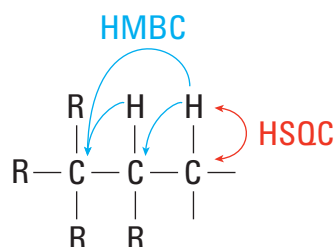
We have all 27 carbons associated with two large substructures and three degrees of unsaturation remain to be assigned.



### 8. Determine the long-range $^1\text{H}$ - $^{13}\text{C}$ connectivities—gradient Heteronuclear Multiple Bond Coherence (gHMBC)

The lack of structural completeness from fragments containing quaternary carbons is to be expected from our primary use of the proton-bearing indirect detection techniques. Long-range (multiple-bond)  $^1\text{H}$ - $^{13}\text{C}$  correlations can be used to bridge the quaternary carbons and link the identified structural fragments. The current structure has two fragments which need to be joined, and contains

eight linkage points. In a typical molecule,  $^2\text{J}_{\text{CH}}$  and  $^3\text{J}_{\text{CH}}$  are commonly seen. In aromatic, conjugated, or cyclic systems with multiple electronic bonding pathways between atoms,  $^4\text{J}_{\text{CH}}$  are often seen. The gHMBC experiment correlates  $^1\text{H}$ - $^{13}\text{C}$  chemical shifts through long-range  $^n\text{J}_{\text{CH}}$  couplings where  $n = 2, 3, 4,$  and above.



The gHMBC spectra provided for protons 6a and 6b (Figure 21) shows long-range correlations to carbons 1 and 3. Proton 4 shows long-range correlations to carbons 1, 2, 3 and a 4-bond correlation to 6. This forms one of the three rings required for the structure and eliminates two linkage points.

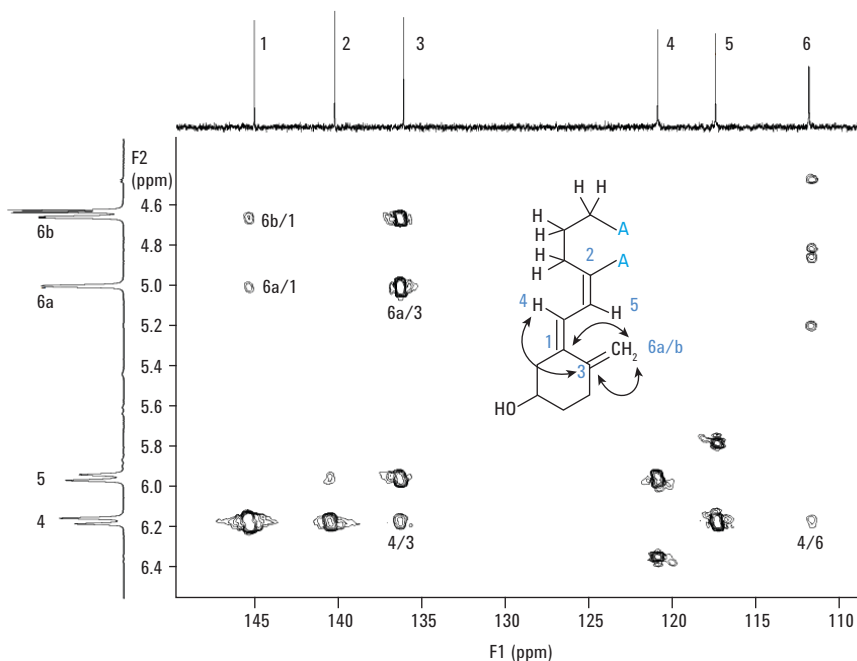


Figure 21. The gHMBC experiment shows clear correlations from the carbon identified as number 1 to the protons identified as 6a and 6b and from carbon 3 to proton 4, closing the ring for the upper of the substructures shown in the TOCSY figure above.

The two fragments can be linked together by noting the correlations between proton 9 with carbons 2 and 5, (Figure 22). The four remaining linkage points must form two rings.

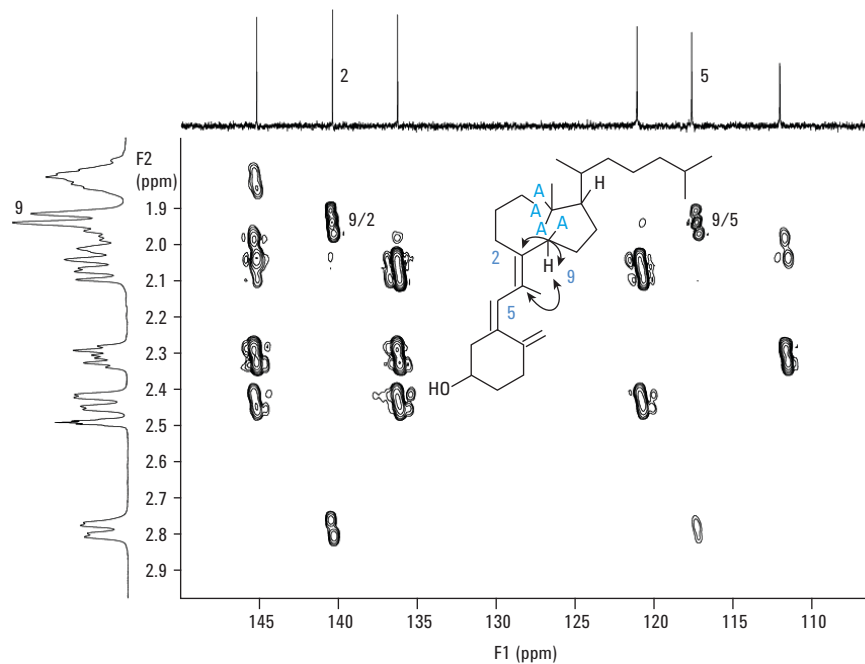


Figure 22. This gHMBC expansion shows how the two fragments are connected.

The long-range correlations from the singlet methyl 27 to carbons 8, 9, 11, and 12 (arrows to 12 and 9 shown) complete the 2-dimensional structure.

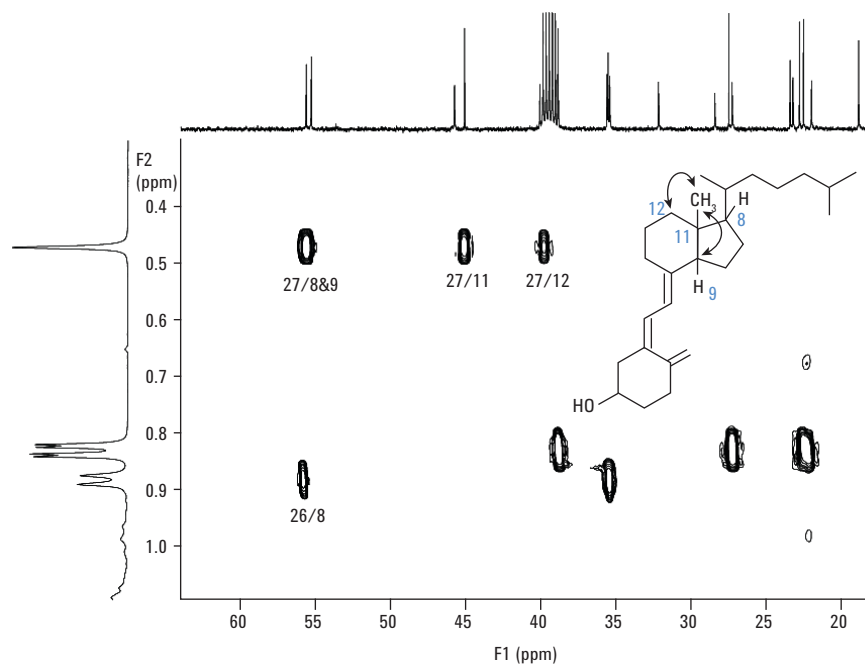


Figure 23. The complete 2D structure is determined through the correlations shown here, which close the final ring.

## Here is what we know from the gHMBC experiment

We have a complete 2 dimensional structure of the unknown compound.

What is important to note is the gHMBC experiment contains much information that can be used to confirm previous assignments, those from the gCOSY and TOCSY type experiments.

The relative stereochemistry of each stereogenic center remains to be assigned. There are five stereogenic centers, leading to 32 possible stereoisomers. NMR is able to reduce the possibilities to two, which would be enantiomers.

## 9. Assigning stereochemistry - Rotational Overhauser Effect Spectroscopy (ROESY)

Once the primary assignments have been made, it is often possible to establish relative stereochemistry with the observation of a few well chosen nuclear Overhauser effect (nOe) or rotating-frame Overhauser enhancement (rOe) interactions.

The 1-D DPFGE-ROESY experiment shows two significant enhancements indicating that methyl 26 and proton 12a (1.91 ppm) are close in space to the methyl singlet 27. This quick experiment has already assigned two stereogenic centers, and assigned 12a as an equatorial proton.

It is just as quick to assign the geometry of vinyl protons 4, 5, 6a and 6b as shown in the 1-D ROESY spectrum (Figure 25), where proton 6b was selectively excited.

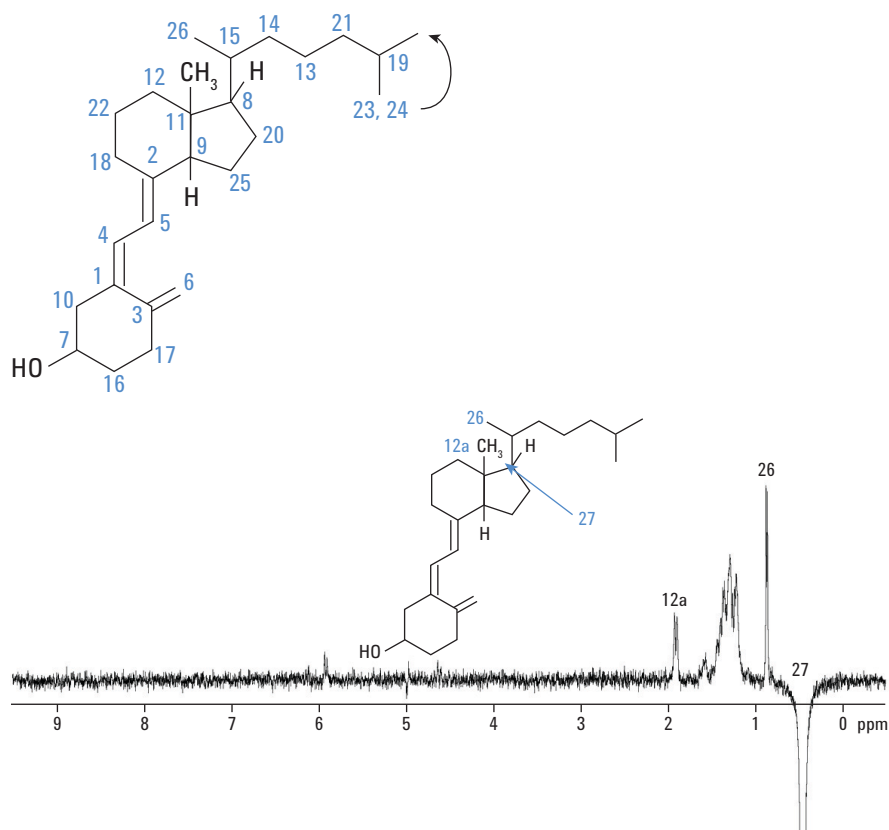


Figure 24. Stereochemical assignments are straightforward to view using the 1-D DPFGE-ROESY experiment.

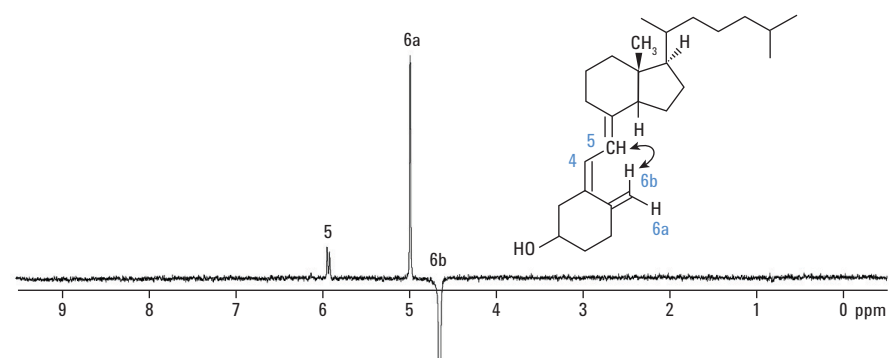


Figure 25. Proton 6b is close in space to protons 5 and 6a – which fixes the geometry of the vinylic region.

The 2-D ROESY spectrum, Figure 26, allows for complete assignment of the relative stereochemistry for the bicyclic ring system. Methine 15 has correlations to methyl 27 and methylene 20a. Methine 8 has a correlation to methine 9.

To establish the relative stereochemistry of the hydroxyl moiety, a key enhancement was observed between 18a and 10a. Without observing this enhancement, the stereochemistry of both cyclic systems could not have been related.

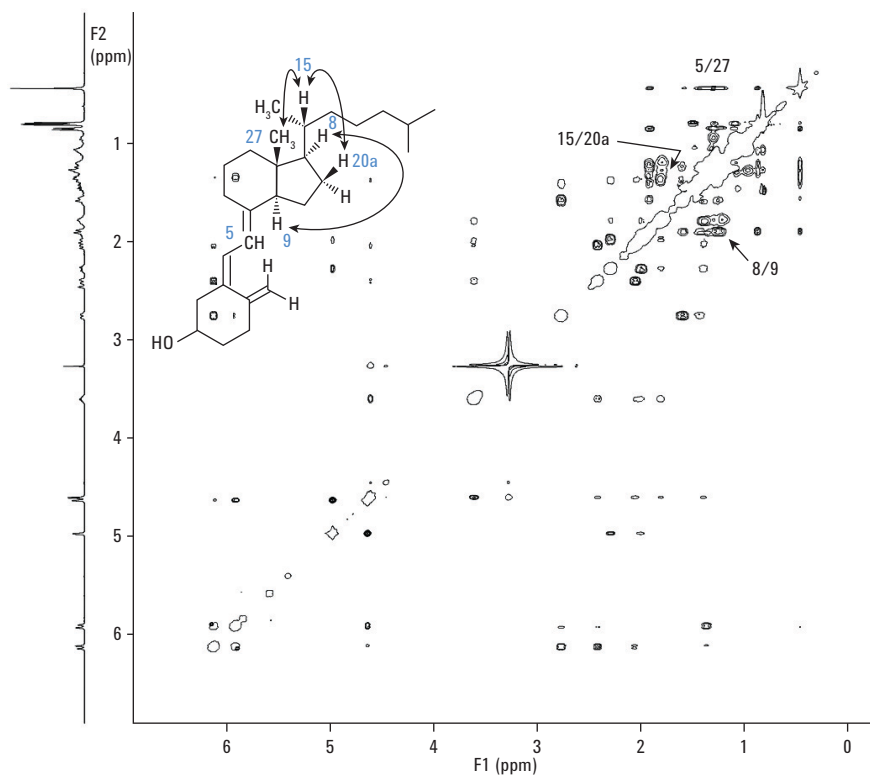


Figure 26. The ROESY experiment is available in a 2D-version.

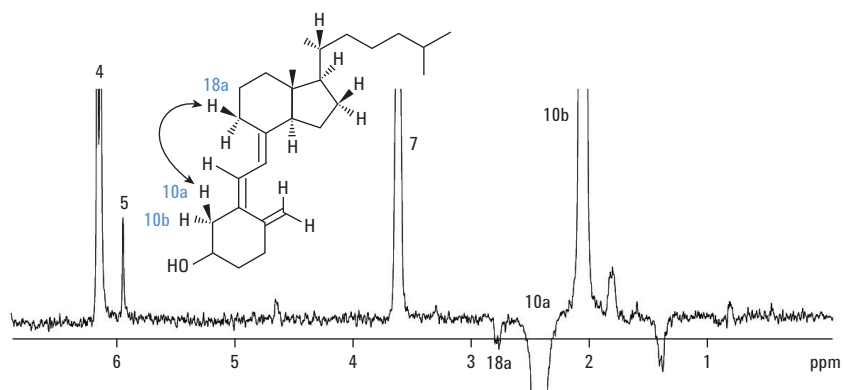


Figure 27. The stability of the Agilent 400-MR system is shown by this demanding experiment which correlates the long range, through-space coupling between the protons 10a and 18a.

The relative stereochemistry of the hydroxyl moiety can then be easily assigned from the 2-D ROESY spectrum, (Figure 28).

## 10. Conclusion

The standard Agilent 400-MR system has all the features necessary – high performance RF, excellent sensitivity and resolution to complete this demanding suite of experiments, providing high quality data throughout. All experiments, including all instrument calibrations and data acquisition is easily achievable in 8–10 hrs. Even more importantly, after the set of experiments is queued, the acquisition process is fully automatic. Assignment, while requiring correlation between different data sets, is not overly demanding due to the informative nature of the experiments; and often becomes a relatively straightforward bookkeeping exercise.

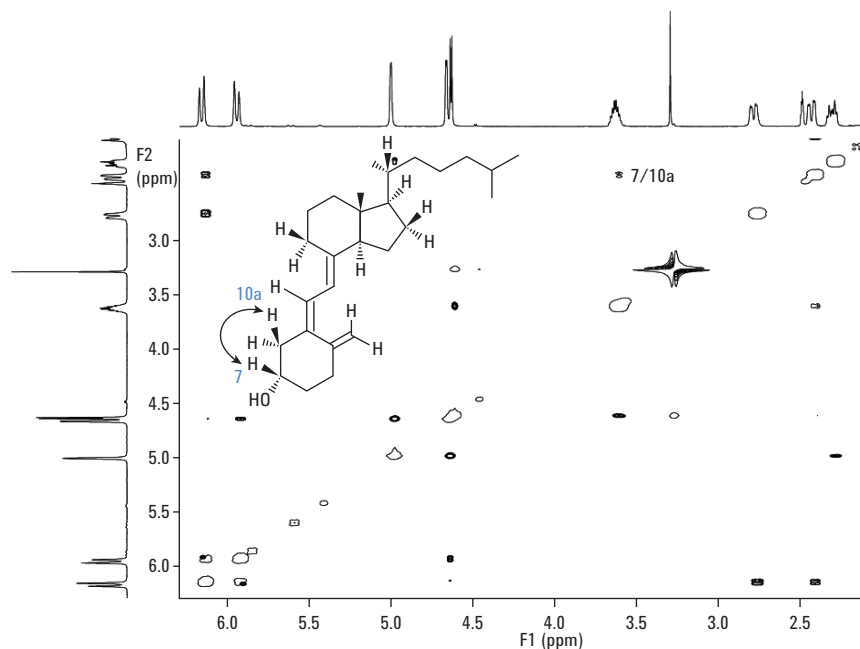
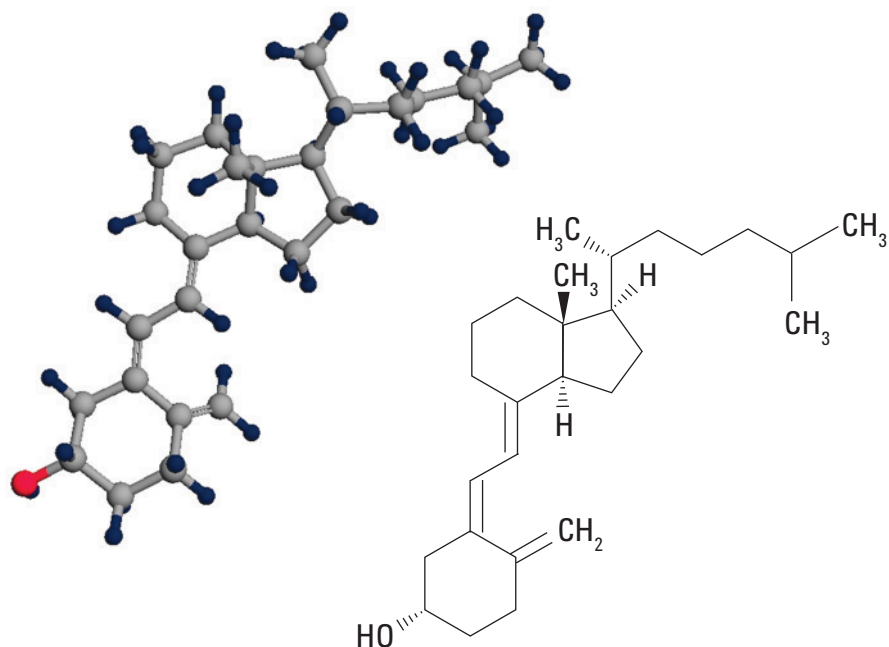


Figure 28. Knowledge of the stereochemistry of 10a allows that of proton 7 to be assigned, thereby assigning the stereochemistry of the hydroxyl group.



[www.agilent.com/chem/nmr](http://www.agilent.com/chem/nmr)

This information is subject to change without notice.

© Agilent Technologies, Inc., 2011  
Published in the USA, December 20, 2011  
5990-9600EN



**Agilent Technologies**